Analysis of Stiffened Curved Panels Under Shear and Compression

M. A. MELCON* AND A. F. ENSRUD†

Lockheed Aircraft Corporation

SUMMARY

This paper presents a method of analysis for curved panels reinforced by longitudinal stiffeners subjected to shear and compression. New formulas have been derived for the critical buckling stress of curved panels in shear and for the various effects of the diagonal tension field in the postbuckling state of the sheet. These latter effects are expressed by fictitious compressive stresses in the stiffeners which are then combined by an interaction equation with the compression stresses due to the external loading. In addition, a formula is given for the ultimate shear strength of the sheet. The method proposed in this paper has been compared with available experimental data, and satisfactory agreement is found. The method has been put in a form that requires the solution of certain mathematical relations and a minimum of chart reading and, hence, is readily adaptable to IBM or other high-speed computing techniques. A sample interaction diagram is included showing how the results of this method may be presented for practical application.

INTRODUCTION

IN SPITE OF GREAT ADVANCEMENTS in the design of aircraft structures, the analysis of stiffened shells still presents a challenging problem. The difficulty arises mainly from the fact that no practical mathematical treatment of the stress pattern in the postbuckling state has been developed as yet. Therefore, for the time being, the designer has to be satisfied with semi-empirical solutions that show sufficient agreement with test results.

Based on a study of the available literature giving theoretical and experimental data pertaining to this subject, a method has been developed for the prediction of the ultimate strength of sheet and longitudinal stiffeners in a curved panel.

NOTATION

A_{st} = stiffener area
a = ring spacing
b = stiffener spacing
C_r = rivet factor, ratio of net to gross area of web
F_c' = allowable compression stress for stiffener alone; F_c' is the lower of either the column allowable (use a fixity of 2 for stiffeners continuous across rings) or the crippling cutoff of the stiffener
F_c = allowable compression stress for stiffener plus effective skin
f_c' = effective compression stress in stiffener due to diagonal tension
f_c'' = a measure of stiffener bending stiffness required to break up shell into panels
f_c = applied compression stress based on stiffener area plus effective width of skin
f_{cg} = applied compression stress based on stiffener area plus total area of skin
F_s = Allowable gross area shear stress for web failure.
F_{so} = basic allowable gross area shear stress (for homogeneous diagonal tension field at 45°)
F_s' = critical buckling shear stress for shell
F_s'' = critical buckling shear stress for flat panel
$F_{scr.}$ = $F_s' + F_s''$ = critical buckling shear stress for curved panel
F_{su} = ultimate shear stress of the material
f_s = applied gross area shear stress
f_{sDT} = part of applied shear stress carried in diagonal tension
F_{tu} = ultimate tensile stress of the material
I_{st} = moment of inertia of stiffener about centroidal axis parallel to the tangent of the skin contour
J_{st} = torsional stiffness factor: for open sections, $J = A_{st}t_{st}^2/3$; for closed sections $J = 4A^2t_{st}/p$, where A is the enclosed area and p is the perimeter
S = shell parameter
R = radius of curvature of panel
t = thickness of web
t_{st} = thickness of stiffener
ν = a factor reflecting the various effects of the diagonal tension field on the stiffener
η = a factor indicating the intensity of diagonal tension in web
λ = a factor reducing the critical shear stress under combined loading

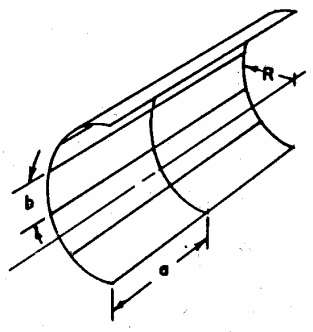

FIGURE 1.
TYPICAL SHELL STRUCTURE

Presented at the Structures Session, Twentieth Meeting, I.A.S., January 28–February 1, 1952, New York. Revised and received August 27, 1952.

* Group Engineer, Structural Methods and Dynamics.
† Structures Engineer.

Method of Analysis

A semimonocoque shell reinforced by rings and longitudinal stiffeners (Fig. 1) may fail in three ways: (1) failure of stiffeners, (2) failure of sheet, and (3) failure of rings. If several components fail simultaneously, the type of failure is usually referred to as general instability. It is assumed that the attachments between skin and supporting members will not shear or pop and thus reduce the ultimate load carrying capacity of the structure.

The following deliberations are limited to an investigation of the first two types of failure. The results of this investigation are then checked against the test data of specimens that failed by buckling of stiffeners or tearing of the skin. Formulas derived in this paper apply specifically only to thin-walled shells of circular cross section with constant values for shear flow, stiffener area, stiffener spacing, and sheet thickness. Adaptations for variation in these items are easily made.

The proposed method may be outlined as follows:

The critical buckling stress of a curved panel is given as the sum of the strength of the shell and that of the panel. If the applied shear stress is below the critical shell-buckling stress, no longitudinal stiffeners are required. On the other hand, it is obvious that the stiffeners must have a certain amount of bending stiffness in order to subdivide the shell into panels. As soon as the applied shear exceeds the critical buckling stress for a curved panel, a rather complex interaction between sheet and supporting members is started. The mathematical treatment becomes extremely involved, if not impossible.

At the start, the shell between the rings bows outward like a barrel. With increasing shear flow, the radial components of the diagonal tension field will pull the stringers inward. In addition, a nonlinear relationship between the applied torque and the compressive stress in the stiffeners can be observed. Failure usually occurs from an individual buckle in the shell forcing the stiffener out of its original location, thus bringing about its collapse by an intricate beam-column action.

Critical Shear Buckling Stress

A simplified expression has been derived for the critical buckling stress of a curved panel. For a flat panel the critical buckling stress may be expressed by

$$F_s'' = KE(t/b)^2 \tag{1}$$

where the magnitude of the coefficient K depends on the material, the degree of edge restraint, and the aspect ratio of the panel. For aluminum alloys and standard construction, this value is taken equal to 5.25 irrespective of aspect ratio. The variation in panel length is taken care of in the term that reflects the effect of curvature. The critical buckling stress of the curved panel may be expressed by

$$F_{s_{cr.}} = KE(t/b)^2$$

where in this case $K = 5.25 + (\pi/4)(b/a)^2 S^{3/4}$ and $S = a^2/Rt$ denotes the shell parameter. This formula for the critical buckling stress of a curved panel may be transformed to the form

$$F_{s_{cr.}} = F_s' + F_s'' \tag{2}$$

where

$$F_s' = (\pi/4\sqrt[4]{S})(Et/R)$$
$$F_s'' = 5.25E(t/b)^2$$

Postbuckling Behavior of a Shear Panel

With the introduction of thin sheet construction for aircraft structure, engineers began to accept the new idea that the buckling of structural components did not necessarily indicate failure. Since that time, a great deal has been written on the postbuckling behavior of structures. Of foremost importance in the study of this subject, is the theory of the incomplete diagonal tension field.

The stress pattern in a flat sheet subjected to shear forces beyond its buckling strength is known as diagonal tension. A rigorous formulation of the transition from the unbuckled state to Wagner's[7] ideal diagonal tension field has not yet been accomplished. Semiempirical formulas developed by Kuhn[8] are most widely used.

When the stress in a plane web starts to exceed its initial buckling strength, the applied shear forces are gradually taken by a combined truss action of the web and stiffeners. The sheet acts more and more like a diagonal, while the stiffeners take the place of uprights. There is a tendency for a buckle to form from corner to corner of the panel, provided this pattern is compatible with the deformation of the stiffeners supporting the edges of the panel.

The various methods proposed for the analysis of flat panels in the postbuckling state differ in the assumption of magnitude of compression stress the sheet is able to sustain in its buckled shape. Additional complications arise when the panel is curved. The diagonal tension in the sheet tends to reduce its curvature in the direction of the wrinkles. This action induces nonuniform radial loads on the longitudinal stiffeners.

Analysis of Longitudinal Stiffeners

The longitudinal stiffeners in a reinforced shell perform three functions: (1) They subdivide the shell into panels; (2) they sustain axial and radial loads induced by the tension field; and (3) they sustain directly applied axial loads. As long as the shell stiffened by rings only is able to sustain the applied shear flow without buckling, no stiffeners are required for the purpose of reducing the panel size. With increasing shear flow, it usually becomes more desirable to raise the initial buckling stress by the addition of longitudinal stiffeners than by thickening of the shell. The required bending stiffness of the stiffeners which will raise the initial

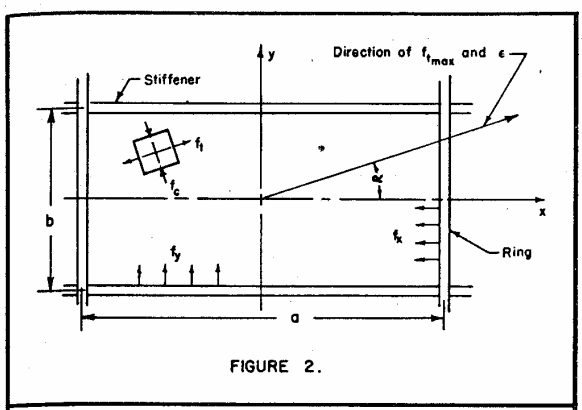

FIGURE 2.

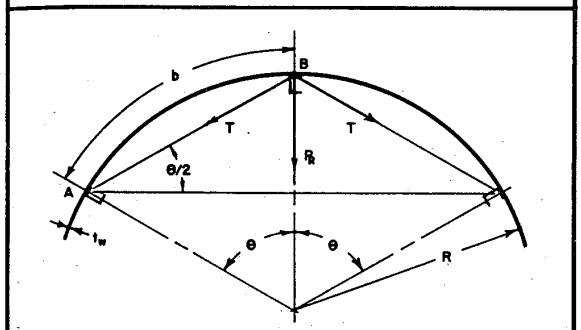

FIGURE 3.

buckling stress to the full value of shell plus panel may be determined according to Seydel's[10] formula for the critical shear stress of flat orthotropic plates,

$$F_{s_{cr.}} = (32/ta^2)\sqrt[4]{D_1D_2^3}$$

where

$$D_1 = D$$
$$D_2 = EI_{st}/b$$
$$D = Et^3/12(1 - \mu^2)$$

Setting this expression equal to F_s'' and eliminating on both sides, there follows the expression for the portion of the moment of inertia, ΔI_{st}, of the stiffener required to divide the shell into panels,

$$\Delta I_{st} = (bt^3/5)(a/b)^{3/2}$$

As mentioned previously, this requirement will be transformed into a fictitious compression stress indicating the portion of the stiffener strength needed for effective subdivision into panels. It is assumed that the ratio of the stiffener moment of inertia required for this purpose to its total moment of inertia may be taken equal to the ratio of an additional area to the total area of the stiffener. The following relation for the fictitious compression stress f_c'' is established:

$$f_c''A_{st} = F_c'\Delta A_{st}$$

Then,

$$f_c'' = F_c'\frac{\Delta A_{st}}{A_{st}} = F_c'\frac{\Delta I_{st}}{I_{st}}$$

where $F_c' = \pi^2EI_{st}/a^2A_{st}$ reflects the column strength of the stiffener. Combining and solving these equations gives

$$f_c'' = F_s''(at/A_{st})\sqrt[3]{0.053b/a} \qquad (3)$$

This equation indicates that heavy skin and wide ring spacing require strong stiffeners in order to avoid excessive values of f_c''. However, this portion of the total effective compression stress in the stiffener in most structures is usually small.

The effects of the diagonal tension field on the stiffeners in a buckled shell are rather complex. The axial load build-up in the longitudinal stiffeners caused by the diagonal tension (Fig. 2) is given by

$$P = (f_s - F_{s_{cr.}})bt \cot \alpha$$

In addition, there are radial components of the diagonal tension field which produce bending moments in the stiffeners. The pull per running inch (Fig. 3) exerted by the tension field along this chord line is

$$T = (f_s - F_{s_{cr.}})t \tan \alpha$$

and the radial load per running inch is

$$P_R = Tb/R = (f_s - F_{s_{cr.}})bt(\tan \alpha/R)$$

The unknown angle α may be found by trial and error. However, this standard approach to the analysis of longitudinal stiffeners does not agree with tests for many reasons, and, hence, a different approach to the problem was chosen.

Fig. 4 pictures a stiffened shell subjected to torsion. Assuming a diagonal tension field of 45° and no bending in the stiffeners, the induced compression stress in the stiffeners is given by

$$f_c' = (f_s - F_{s_{cr.}})(bt/A_{st}) \qquad (4)$$

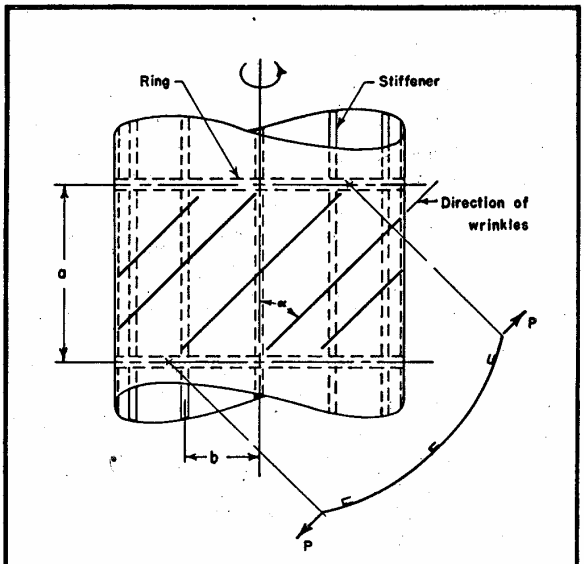

FIGURE 4.

The actual angle of the tension field is usually smaller than 45°; in addition, there is a pull P along the direction of the wrinkles which forces the stringers toward the center of the cylinder. It can be seen from Fig. 4 that the pull P has a greater effect on stringers of smaller flexibility, because the shell support in this case starts at a later state. Furthermore, it is obvious that this effect is increased with sharper curvature. These, in addition to other considerations, led to the determination of the empirical factor ν, which was introduced into Eq. (4) to give a fictitious compression stress that is a measure of required stiffener strength to sustain the effects of diagonal tension. Eq. (4) then transforms into

$$f_c' = \nu(f_s - F_{s_{cr.}})(bt/A_{st}) \tag{5}$$

where

$$\nu = 1 + (a/R)\sqrt[4]{(I_{st}/J_{st})(t/b)}$$

This formula gives satisfactory results for shells with $R \leqslant 100$ in. The total effective or fictitious compression stress for which the stiffener must be designed becomes, then,

$f_c' + f_c''$ = total effective compression stress in stiffener

The allowable stress to be used for determining the strength of the stiffener is F_c', which is the lower of the column allowable (using a fixity of 2 for stiffeners that are continuous across rings) or the crippling cutoff for the stiffener alone. Allowables determined from tests on the stiffener by itself may often be unsuitable for this analysis, since the stiffener may fail in a mode not possible for a stiffener that is attached to the shell. Table A summarizes the effective compression stress to be used at different values of f_s when the panel is subjected to shear alone.

TABLE A

f_c' and f_c'' When Panel Is Subjected to Shear Only

f_c'	f_c''
$f_c' = 0$, when $f_s < F_{s_{cr.}}$	$f_c'' = 0$, when $f_s < F_s'$
$f_c' = \dfrac{\nu(f_s - F_{s_{cr.}})bt}{A_{st}}$, when $f_s \geqslant F_{s_{cr.}}$	$f_c'' = \left(\dfrac{f_s - F_s'}{F_s''}\right)\left(\dfrac{F_s''at}{A_{st}}\right) \times \sqrt[3]{\dfrac{0.053b}{a}}$, when $F_s' \leqslant f_s < F_{s_{cr.}}$
	$f_c'' = \dfrac{F_s''at}{A_{st}} \sqrt[3]{\dfrac{0.053b}{a}}$, when $f_s \geqslant F_{s_{cr.}}$

If, in addition to shear, the panel is also subjected to direct compression, the effects of shear on the stiffener are combined by an interaction equation with the effects of the direct compression. The only exception to the method as previously outlined for determining the effects of shear on the stiffener is that the critical shear buckling stresses, in this case, must be reduced because of the effects of compression. There are well-known interaction equations that give the initial buckling of panels under combined loadings. However, for the purpose at hand, these equations are not satisfactory, since they will not properly account for the amount of the shear being carried in diagonal tension nor will the angle of diagonal tension be the same as when the sheet buckled under shear alone. In other words, it would be conservative to assume that, after buckling occurs in combined shear and compression, any additional shear is carried in the same manner as if the buckling were due to shear alone. If linear interaction were assumed for initial buckling in compression and shear, the following equation may be written:

$$(f_s/F_{s_{cr.}}) + (f_{cg}/F_{c_{cr.}}) = 1$$

Then the shear stress at which the panel buckles becomes

$$f_s = \frac{1}{1 + (f_{cg}/f_s)(F_{s_{cr.}}/F_{cr.})} F_{s_{cr.}}$$

Based on this reasoning, a factor λ was arbitrarily selected to reflect the reduction in the critical shear buckling stress due to compression,

$$\lambda = \sqrt[4]{1/[1 + (f_{cg}/f_s)]} \tag{6}$$

where f_{cg} is the applied compression stress based on stiffener area plus total area of skin.

The prediction of stiffener failure due to the combined action of shear and direct compression is based upon the following interaction equation:

$$\left(\frac{f_c' + f_c''}{F_c'}\right)^{1.125} + \left(\frac{f_c}{F_c}\right)^{1.125} = 1 \tag{7}$$

where f_c is the direct compression stress based on stiffener area plus effective width of skin and F_c is the allowable compression stress based on the same area. In other words, the ratio f_c/F_c is the ratio of the applied compression load to the allowable compression load of the stiffener plus skin. Table B summarizes the effective compression stress to be used at different values of f_s when the panel is subjected to shear and compression. For $\lambda = 1$, Table B is identical with Table A.

TABLE B

f_c' and f_c'' When Panel Is Subjected to Shear and Compression

f_c'	f_c''
$f_c' = 0$, when $f_s < \lambda F_{s_{cr.}}$	$f_c'' = 0$, when $f_s < \lambda F_s'$
$f_c' = \dfrac{\nu(f_s - \lambda F_{s_{cr.}})bt}{A_{st}}$, when $f_s \geqslant \lambda F_{s_{cr.}}$	$= \left(\dfrac{f_s - \lambda F_s'}{F_s''}\right)\left(\dfrac{\lambda F_s''at}{A_{st}}\right) \times \sqrt[3]{\dfrac{0.053b}{a}}$, when $\lambda F_s' \leqslant f_s < \lambda F_{s_{cr.}}$
	$f_c'' = \dfrac{\lambda F_s''at}{A_{st}} \sqrt[3]{\dfrac{0.053b}{a}}$, when $f_s \geqslant \lambda F_{s_{cr.}}$

Little test data could be found for shells reinforced by stiffeners with closed section. Whether the factor ν still applies in this case could therefore not be substantiated by comparison with test data. The only

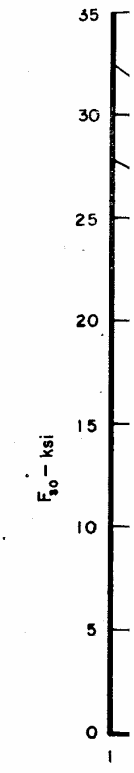

two specime
ing of the v

Analysis of

The form
presented h
net area of
cent of its
the web, th
equal to th
ultimate te
the ultimat
dicates a m
the ideal te
of the sheet
sion of the s
indicates th
cannot deve
terial. The
shear stress
correction i
ferent from
corner of th
empirical fa

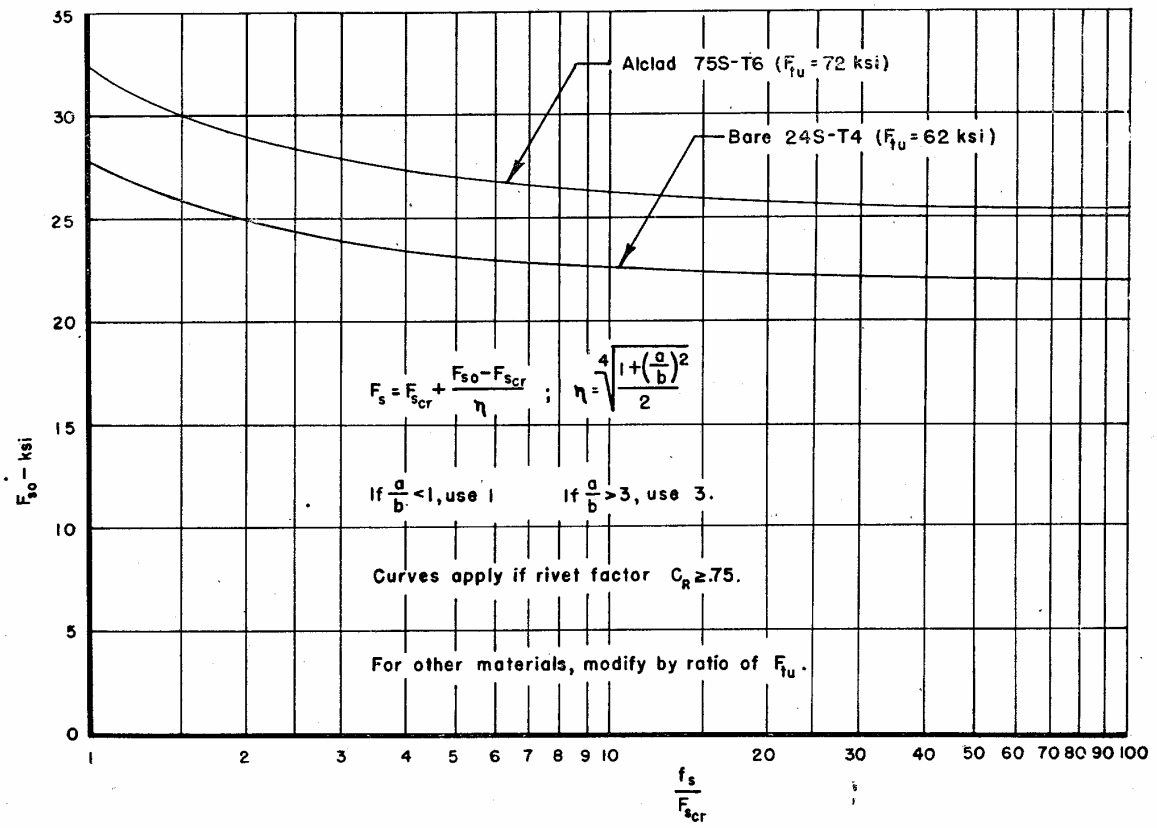

FIGURE 5 - ULTIMATE ALLOWABLE GROSS AREA SHEAR STRESS.

two specimens that had closed stiffeners failed by tearing of the web.

Analysis of Shear Web

The formulas for the allowable gross area shear stress presented here are based on the assumption that the net area of the sheet is equal to, or greater than, 75 per cent of its gross area. In the unbuckled condition of the web, the maximum tension stress in the sheet is equal to the shear stress. For aluminum alloys, the ultimate tensile strength is approximately 1.67 times the ultimate shear strength of the material. This indicates a marginal tension capacity of 67 per cent. In the ideal tension field, where the compression strength of the sheet is assumed equal to zero, the maximum tension of the sheet is equal to twice the shear stress. This indicates that in the homogeneous tension field the sheet cannot develop the ultimate shear strength of the material. The curve of Fig. 5, giving the basic allowable shear stress F_{so}, takes account of this. However, a correction is also needed to provide for an angle α different from 45° and for wrinkles forming from corner to corner of the panel. This correction is reflected by the empirical factor

$$\eta = \sqrt[4]{[1 + (a/b)^2]/2}$$

if $a/b < 1$, use 1; if $a/b > 3$, use 3. The ultimate allowable gross area web stress is, therefore,

$$F_s = F_{s_{cr.}} + [(F_{so} - F_{s_{cr.}})/\eta] \qquad (9)$$

where F_{so} is obtained from Fig. 5.

The curves of Fig. 5 are similar to the lower curves of reference 11, Fig. 9. The curves of this reference were modified so that for $f_s/F_{s_{cr.}} = 1$ the basic allowable shear stress becomes $F_{so} = 0.75F_{su}$. This correction is made so that net area shear stress will never exceed F_{su}.

In exceptional cases where the net area of the sheet is less than 75 per cent of the gross area, an additional check is recommended. The circular interaction for combined tension and shear is given by the formula

$$\left[\frac{f_s}{C_R F_{su}}\right]^2 + \left[\frac{\eta(f_s - F_{s_{cr.}})}{C_R F_{tu}}\right]^2 = 1 \qquad (10)$$

where C_R denotes the rivet factor.

If compression is superimposed on the shear stress in the panel, the initial buckling stress is again multiplied by the factor λ in both Eqs. (9) and (10).

Analysis of Attachments

At either end of the sheet or at splices, the load in the sheet must be transferred by rivets or fasteners to other

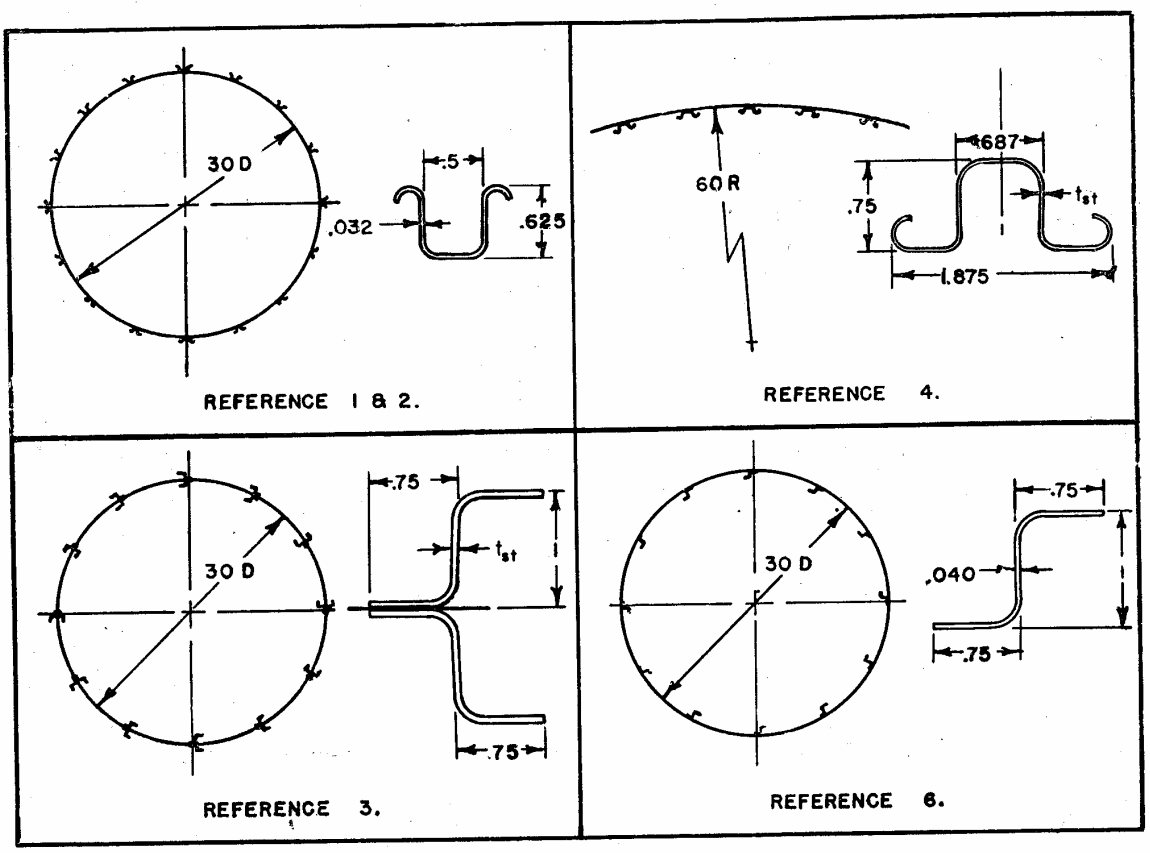

FIGURE 6 - TYPES OF SPECIMENS TESTED

parts of the structure. The shear load for which each fastener should be checked is given by

$$P = qp\sqrt{1 + \left[\frac{\eta(f_s - F_{s_{cr.}})}{f_s}\right]^2} \qquad (11)$$

where p = pitch of fasteners and q = shear flow in sheet. Again, reduce $F_{s_{cr.}}$ by the factor λ if compression is present.

Comparison with Test Data

The substantiation for the methods proposed herein are based upon the test work performed by the N.A.C.A.[3,6], the Aluminum Company of America,[1,2] Douglas Aircraft Company, Inc.,[4] and the National Bureau of Standards.[5] A sum total of 54 test specimens has been analyzed in this investigation. Fig. 6 shows the general configurations of the types of specimens tested. As can be observed, some of the specimens are complete cylinders stiffened with longitudinal stiffeners and rings, while others are portions of cylinders. The radius of specimens varied from 15 to 60 in.; skin gage, from 0.020 to 0.051; and the factor ν had a range on the specimens examined from approximately 1.10 to 3.

Critical Buckling Shear Stress

Table 1 gives a comparison of the critical buckling shear stress computed by the method of this paper, by the method of reference 9, and observed test values. Twenty-six panels were checked. Test values averaged 2.0 per cent higher than predicted by the proposed method and 5.8 per cent higher than by the method of reference 9. Figure 7 shows graphically the relationship between test and predicted values. There is no significant difference between the predictions of the two methods. The advantage of the proposed method lies in the fact that the buckling stress of the curved panel is expressed explicitly in terms of parameters of the panel and that reference to charts is not required.

Panels Subjected to Shear Only (Stiffener Failures)

A total of 24 specimens that were subjected to shear only failed in the stiffener. Fig. 8 shows the relationship between the shear strength predicted by the method of this paper and test shear strength. Including all specimens, the average conservatism of the prediction is 7.8 per cent. The results from specimen 2 of reference 2 and specimen 10 of reference 4 were overly conservative. In the first case the stiffener apparently

TABLE 1

Comparison of Initial Buckling Stress Computed by $F_{scr.} = F_s' + F_s''$ by Method of Reference 9 and Observed Test Values. Panels Subjected to Shear Only

Reference	Specimen	Initial Buckling Stress: Proposed method, $F_{scr.} = F_s' + F_s''$	Initial Buckling Stress: Method of ref. 9	Initial Buckling Stress: Observed by test	Ratio of Test to Predicted: Proposed method	Ratio of Test to Predicted: Method of ref. 9
1	14	2,869	2,840	2,950	1.028	1.039
	20	2,844	2,750	2,870	1.009	1.044
	21	3,455	3,230	4,120	1.192	1.276
2	2	3,018	3,160	3,460	1.146	1.095
	5	4,128	3,730	4,130	1.000	1.107
	8	4,854	4,480	4,660	0.960	1.040
	11	5,442	5,400	5,160	0.948	0.956
	3	4,245	4,790	4,720	1.112	0.985
	6	5,580	5,700	6,040	1.082	1.060
	9	5,755	5,480	5,840	1.015	1.066
	12	6,710	6,120	7,150	1.066	1.168
3	1	3,318	2,950	3,200	0.964	1.085
	2	4,897	4,580	5,000	1.021	1.092
	3	3,643	3,480	3,700	1.016	1.063
	4	4,908	4,600	4,800	0.978	1.043
	5	6,317	6,700	6,400	1.013	0.955
	6	8,383	8,360	8,500	1.014	1.017
	7	7,115	6,530	6,700	0.942	1.026
	8	8,508	8,640	8,800	1.034	1.019
	9	3,939	3,940	3,040	0.774	0.773
	10	2,326	2,350	2,380	1.023	1.014
	11	7,552	7,110	7,900	1.046	1.111
	12	6,472	6,170	7,270	1.123	1.179
4	8	1,480	1,470			
	28	1,212	1,230			
	27	1,480	1,460			
	32	2,200	2,200			
	16	1,212	1,230			
	3	1,480	1,460			
	10	2,200	2,200			
5	20a	14,420	12,780	12,200*	0.846	0.955
	30a	12,258	10,850	13,150	1.073	1.212
6	1	3,418	3,280	3,700	1.083	1.128

* This observed test value is probably low because of some initial condition, since identical panels with larger radii buckled at a higher stress.

developed a fixity of 4 instead of 2 as determined from the compression stresses read in the strain gages, and in the second case the test is questioned, since this specimen was one of a family of specimens and the test results were incompatible with the rest. If these two specimens are excluded, the average conservatism becomes 5.8 per cent.

Panels Subjected to Shear Only (No Stiffener Failures)

As a negative check of the method for predicting stiffener failures, 15 specimens that did not fail in the stiffener were analyzed for stiffener failure. The purpose of this was to determine to what extent stiffener failures would be predicted by the proposed method when they did not actually occur in the test panel. Fig. 9 is a graph of predicted shear stress vs. test shear stress and indicates that for most of the specimens the test stress is lower than the predicted stress. This is as it should be, since these panels did not fail in the stiffener.

Those panels that had a test stress close to the predicted stress based on stiffener failure failed by popping of the rivets, and it is questionable whether the panels would have carried much more stress had the rivets not failed.

Panels Subjected to Combined Shear and Compression (Stiffener Failures)

A total of 15 specimens subjected to shear and compression were analyzed. Fig. 10 shows the interaction between effective compression in stiffener due to shear and the direct compression for the test specimens analyzed.

The results indicate an average conservatism for the method of prediction of 5.0 per cent. The test result from one specimen from reference 4 with a high conservatism was considered to be questionable, since it was not compatible with other tests in the same series of specimens. If this specimen is neglected, the average conservatism drops to 3.8 per cent. The actual conservatism in an interaction diagram between shear flow in skin and compression load on stiffener would be less than the above value, since the conservatism enters into only that portion of the shear flow supported by the stiffeners.

Panels Subjected to Shear Only (Web Failures)

Nine specimens failed in the web. Fig. 11 shows a graph of test stress vs. predicted stress for web failure. The results indicate that the method is conservative by an average of 0.3 per cent. There is reason to question

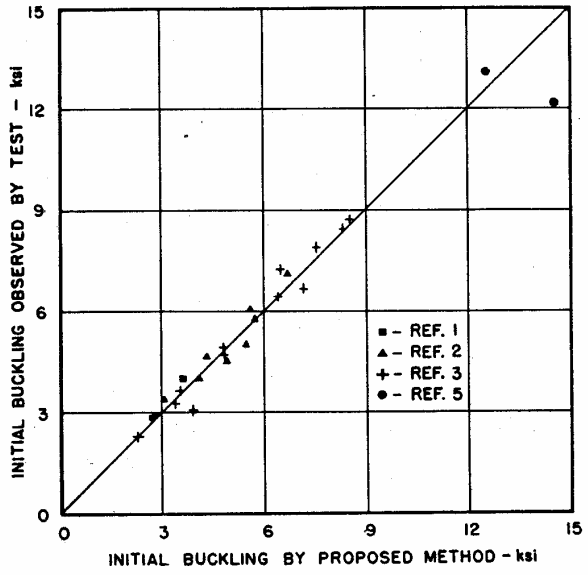

FIGURE 7. - INITIAL SHEAR BUCKLING STRESS IN CURVED PANELS.

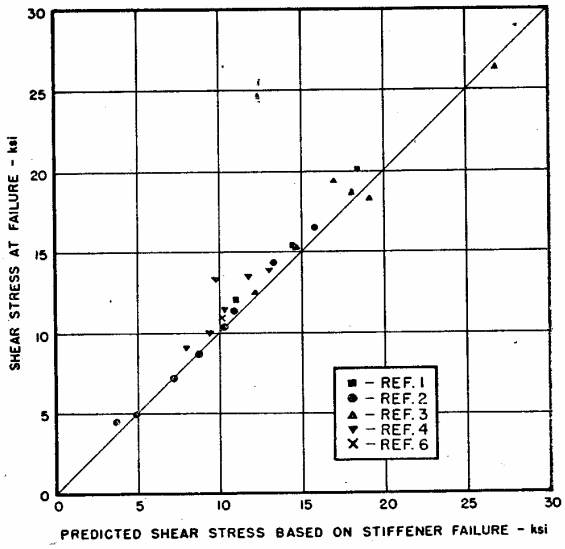

FIG 8 - SHEAR STRESS AT FAILURE vs PREDICTED SHEAR STRESS FOR PANELS WITH STIFFENER FAILURES. PANELS SUBJECTED TO SHEAR ONLY.

the results from three of the specimens. Specimens 20a and 30a of reference 5 failed by tearing the sheet in the end panels and was precipitated by shearing of rivets connecting stringers to jig. In testing specimen 1 of reference 3, the loading jig bound, and the applied torque was actually about 10 per cent greater than the test gage indicated. If these three specimens were omitted, the average conservatism becomes 4.0 per cent.

Typical Application

A typical application to which this method of analysis may be applied is the determination of allowable strengths for a fuselage shell structure. The following is an outline of the procedure for constructing an interaction curve of combined shear and compression on a curved panel. An example of such curves is shown in Fig. 12.

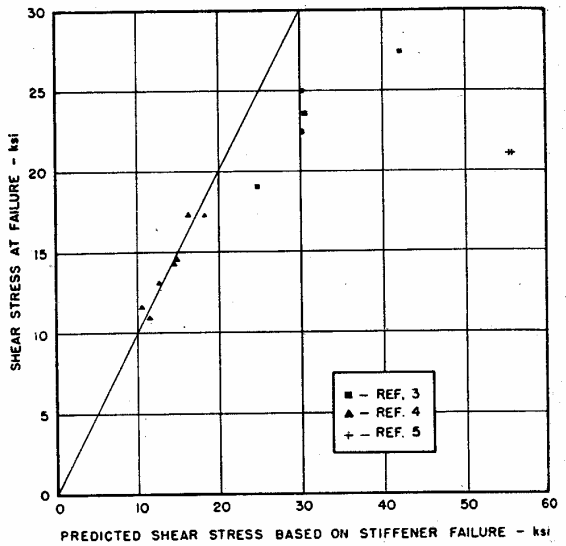

FIG 9 - SHEAR STRESS AT FAILURE vs PREDICTED SHEAR STRESS FOR PANELS WITHOUT STIFFENER FAILURES. PANELS SUBJECTED TO SHEAR ONLY.

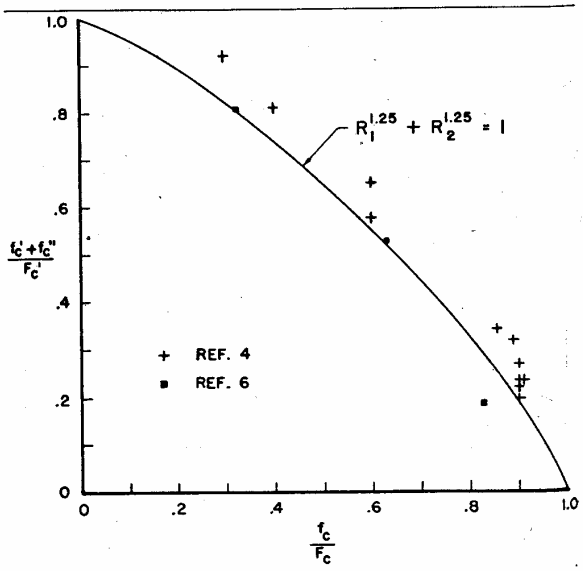

FIGURE 10 - INTERACTION OF COMPRESSION DUE TO SHEAR AND DIRECT COMPRESSION FOR PANELS WITH STIFFENER FAILURES. PANELS SUBJECTED TO SHEAR AND COMPRESSION.

Interaction for Stiffener Failure

(1) The ring spacing, stiffener spacing, stiffener section, skin gage, and the radius of the panel are known; hence, the factor ν may be calculated.

(2) Determine F_c' and F_c. These may be calculated by standard procedures. The allowable compression strength of a panel is often determined as a load per stiffener and skin rather than as a stress on stiffener plus effective skin. For the rest of this example, it will be assumed that P is the allowable compression load and p is the applied compression load.

(3) Assume a value for p.

(4) For the assumed value p, assume several values of f_s and obtain corresponding values of λ from Eq. (6). [λ involves f_{cg}, which is determined by $p/(A_{st} + bt)$.]

(5) From Table B, determine f_c' and f_c'' for assumed values of f_s and corresponding values λ.

(6) Determine value of f_s which makes

$$\left(\frac{f_c' + f_c''}{F_c'}\right)^{1.25} = 1 - \left(\frac{p}{P}\right)^{1.25}$$

(7) This value of f_s times t is then the shear flow that may be applied with the compression load p. Repeat this procedure for other values of p to complete the interaction for stiffener failure.

Interaction of Web Failure

The effect of compression on the ultimate shear strength of the web is small, since its only influence is to reduce the critical buckling shear stress, $F_{s_{cr.}}$, by the factor λ. The web failure curve with the effect of compression included may be obtained as follows:

(1) Compute η.

(2) Perform steps 3 and 4 under section above.

(3) Determine the value of f_s such that $f_s = F_s$, where F_s is given by Eq. (9). It should be noted that in these determinations $F_{s_{cr.}}$ must be multiplied by the factor λ. If the rivet factor $C_R < 0.75$, then an additional check must be made in accordance with Eq. (10). The value f_s times t is then the shear flow that will produce web failure.

The envelope of the stiffener failure curve and web failure curve forms the complete interaction curve for the panel. In plotting the curves, it is recommended that $p = 0$ be the first point investigated, since in this case λ is always equal to one and the trial-and-error solution involved in steps 4, 5, and 6 of the section above is eliminated. Once the value of f_s at $p = 0$ has been determined, it is possible to make a close first approximation as to what f_s will be at other values of p, and again labor of trial and error will be greatly reduced.

Conclusions

(1) Simplified formulas for the calculation of critical shear buckling stress of curved panels have been derived. Test values averaged 2.0 per cent higher than predicted values.

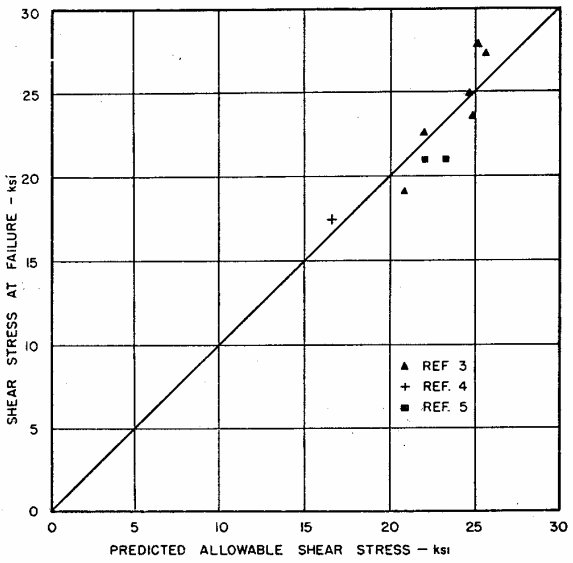

FIGURE 11. - SHEAR STRESS AT FAILURE vs PREDICTED ALLOWABLE SHEAR STRESS FOR PANELS WITH WEB FAILURES. PANELS SUBJECTED TO SHEAR ONLY.

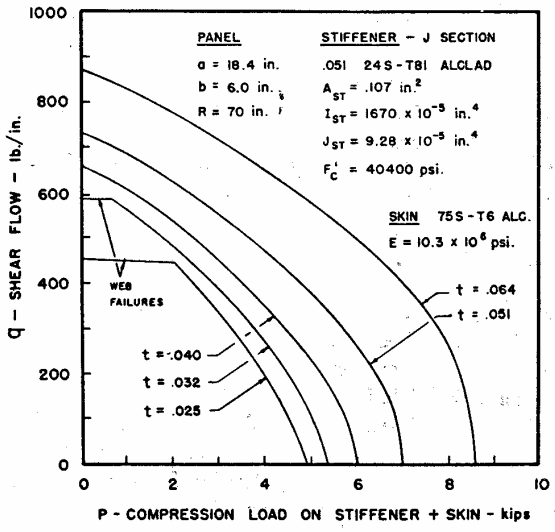

FIGURE 12. - EXAMPLE OF INTERACTION CURVES OF COMBINED SHEAR AND COMPRESSION ON CURVED PANELS.

(2) A method has been determined for predicting the ultimate strength of a stiffened curved panel subjected to shear. The average prediction is approximately 6 per cent conservative for longitudinal stiffener failure and 4 per cent conservative for web failure.

(3) A method has been determined for predicting the ultimate strength of a stiffened curved panel subjected to combined shear and compression. The average prediction is slightly less than 3.8 per cent conservative for longitudinal stiffener failure.

(*Concluded on page 126*)

or

$$\frac{1}{c}\int\int Py\,dS = \frac{U_0}{i\omega c}\int\int \bar{P}w\,dS \qquad (56)$$

The integral on the left side is the rolling moment that gives the required result.

Conclusions

A general relation between linearized solutions of lifting-surface problems in direct and reverse flow has been established for compressible nonsteady flows. This relation is a direct extension of that already known for steady-flow solutions. On the basis of the analysis leading to this result, an adjoint variational principle, also the counterpart of one already known for steady flows, has been established. This may be useful in the approximate solution of lifting-surface problems in nonsteady flow. Several applications of the general theorem to problems in nonstationary wing theory have been given. These included determination of relations between certain aerodynamic coefficients for plan forms in direct and reverse flow and establishment of influence functions for total lift, pitching moment, and rolling moment for wings oscillating with arbitrary motion and deformation of the plan form. The influence functions were found to be certain simple solutions for the plan form in reverse flow.

References

[1] von Kármán, Th., *Supersonic Aerodynamics—Principles and Applications*, Journal of the Aeronautical Sciences, Vol. 14, No. 6, pp. 373–409, July, 1947.

[2] Hayes, W. D., *Linearized Supersonic Flow*, North American Aviation, Inc., Report No. AL-222, June 18, 1947.

[3] Flax, A. H., *Relations Between the Characteristics of a Wing and Its Reverse in Supersonic Flow*, Journal of the Aeronautical Sciences, Vol. 16, No. 8, pp. 496–504, August, 1949.

[4] Munk, M. M., *The Reversal Theorem of Linearized Supersonic Airfoil Theory*, Journal of Applied Physics, Vol. 21, No. 2, pp. 159–161, February, 1950.

[5] Harmon, S., *Theoretical Relations Between the Stability Derivatives of a Wing in Direct and in Reverse Supersonic Flow*, N.A.C.A. T.N. No. 1943, September, 1949.

[6] Brown, C. E., *The Reversibility Theorem for Thin Airfoils in Subsonic and Supersonic Flow*, N.A.C.A. T.N. No. 1944, September 1949.

[7] Ursell, F., and Ward, G. N., *On Some General Theorems in the Linearized Theory of Compressible Flow*, Quarterly Journal of Mechanics & Applied Mathematics, Vol. III, Part 3, pp. 326–348, September, 1950.

[8] Flax, A. H., *General Reverse Flow and Variational Theorems in Lifting-Surface Theory*, Journal of the Aeronautical Sciences, Vol. 19, No. 6, pp. 361–374, June 1952.

[9] Webster, A. G., *Partial Differential Equations of Mathematical Physics*, p. 219; G. E. Steckert & Company, 1933.

[10] Rayleigh, Lord, *Theory of Sound*, Vol. II, pp. 145–147; Dover Publications, Inc., 1945.

[11] Reissner, E., *On the General Theory of Thin Airfoils for Non-Uniform Motion*, N.A.C.A. T.N. No. 946, August, 1944.

[12] Schwartz, L., *Berechnung der Druckverteilung einer harmonish sich verformenden Tragfläche in ebener Strömung*, Luftfahrtforschung, Vol. 17, pp. 379–386, 1940.

[13] Söhngen, H., Schwartz, L., and Dietze, F., Three Papers from Conference on "Wing and Tail Surface Oscillations," Munich, March 6–8, 1941. Also, N.A.C.M. T.M. No. 1306, August, 1951.

Analysis of Stiffened Curved Panels Under Shear and Compression

(*Concluded from page 119*)

References

[1] Moore, R. L., and Wescoat, C., *Torsion Tests of Stiffened Circular Cylinders*, N.A.C.A. Advanced Restricted Report No. 4 E 31, 1944.

[2] Clark, J. W., and Moore, R. L., *Torsion Tests of Aluminum Alloy Stiffened Circular Cylinders*, Unpublished Alcoa Report No. 12-50-15-A, 1951.

[3] Kuhn, Paul, and Peterson, James P., *A Summary of Diagonal Tension*, N.A.C.A. T.N. No. 2662, 1952. (N.A.C.A. T.N. No. 1481, 1947, *Diagonal Tension in Curved Webs.*)

[4] Anderson, P. N., *Combined Compression and Shear in Skin and Stiffener Combinations*. Douglas Aircraft Company Report No. 3021, 1941.

[5] Goodman, Stanley, *Tests of Reinforced Curved Sheet in Shear*, National Bureau of Standards Lab. No. 64180 PRI, 1949.

[6] Peterson, James P., *Experimental Investigation of Stiffened Circular Cylinders Subjected to Combined Torsion and Compression*, N.A.C.A. T.N. No. 2188, 1950.

[7] Wagner, Herbert, *Flat Sheet Metal Girders with Very Thin Metal Web*, N.A.C.A. T.M. No. 606, 1931.

[8] Kuhn, Paul, and Peterson, James P., *Strength Analysis of Stiffened Beam Webs*, N.A.C.A. T.N. No. 1364, 1947.

[9] Batdorf, S. B., *A Simplified Method of Elastic Stability Analysis for Thin Cylindrical Shells*, N.A.C.A. Report No. 874, 1947.

[10] Seydel, E., *The Critical Shear Load of Rectangular Plates*, N.A.C.A. T.M. No. 705, 1933.

[11] Levin, L. R., and Sandler, C. W., Jr., *Strength Analysis of Stiffened Thick Beam Webs*, N.A.C.A. T.N. No. 1820, 1949.

This pa
shear-flow
with nonl
loads. Th
segment a
age rate o
ably separ
is for a wi
monocoqu
loading cor
The she
ponent of
chord she
may be de
sired.
This me
Machine o
on machin
faster Car
by IBM to
flows and c
sultant she
The resu
paper on t
curved surf
the "Unit M

a
A,
c.g.
C_1
C_2
C_3
C_4
E
f
G
h_X
h_Z
I_X, I_Z
I_{XZ}
l.r.a.
Δl
M_X, M_Z
n
N

Received
19, 1952.
* Senior C
† Stress A

The Laurent expansion of Eq. (21) is

$$z = \zeta + (2/n)[(c^n - a^n)/\zeta^{n-1}] + 0(1/\zeta^{2n-1}) \qquad (22)$$

hence for $n \geq 3$, $a_1 = 0$, and

$$m_{12} = m_{13} = m_{23} = 0$$

$$m_{11} = m_{22} = 2\pi\rho \left\{ \left[\frac{b^{n/2} + (a^2/b)^{n/2}}{2} \right]^{4/n} - \frac{a^2}{2} \right\} \qquad (23)$$

already given in reference 7.

If $a = 0$ (no body) the Laurent expansion becomes simply a binomial series of the form:

$$z = \sum_{m=0}^{\infty} \frac{a_{mn-1}}{\zeta^{mn-1}}, \qquad \text{where } a_{mn-1} = \frac{\Gamma[1 + (2/n)]\, c^{mn}}{\Gamma[1 + (2/n) - m]\, m!} \qquad (24)$$

Substituting this expression for a_{mn-1} into Eq. (10) we have

$$b_{ln} = \sum_{m=0}^{\infty} \frac{a_{n(m+l)-1}\, a_{mn-1}}{c^{2m}}$$

$$= \frac{(-1)^l}{\pi^2} \sin^2 \frac{2\pi}{n} \left[\Gamma\left(1 + \frac{2}{n}\right) \right]^2 c^{nl+2} \times \sum_{m=0}^{\infty} \frac{\Gamma[l - (2/n) + m]\Gamma[-(2/n) + m]}{\Gamma(l + 1 + m)m!} \qquad (25)$$

where use has been made of the relation $1/\Gamma(1 - z) = (\sin \pi z \div \pi)\, \Gamma(z)$.

This series is a hypergeometric series with argument unity which possesses a closed form sum,[8] so that Eq. (25) can be written as

$$b_{ln} = \frac{(-1)^{l+1}}{\pi} \sin \frac{2\pi}{n}\, \Gamma\left(1 + \frac{4}{n}\right) c^{nl+2} \frac{\Gamma[l - (2/n)]}{\Gamma[l + (2/n) + 1]} \qquad (26)$$

Substituting this latter expression into Eq. (17), we have:

$$m_{33} = \frac{\rho b^4}{2^{8/n}\pi}\, n \sin^2 \frac{2\pi}{n} \left[\Gamma\left(1 + \frac{4}{n}\right) \right]^2 \times \sum_{l=1}^{\infty} \frac{l}{[l + (2/n)]^2} \left\{ \frac{\Gamma[l - (2/n)]}{\Gamma[l + (2/n)]} \right\}^2 \qquad (27)$$

since $c = b/2^{2/n}$.

Eq. (27) can be summed for $n = 1, 2, 4, \infty$, yielding values already found for these cases (reference 9), namely,

$$m_{33} = \rho b^4 \begin{cases} 9\pi/128 \\ \pi/8 \\ 2/\pi \\ \pi/2 \end{cases}; \qquad n = \begin{cases} 1 \\ 2 \\ 4 \\ \infty \end{cases} \qquad (28)$$

where, for $n \to \infty$, use is made of the asymptotic expression for the Γ function, so that the series in Eq. (27) becomes a Riemann Zeta Function:

$$\sum_{l=1}^{\infty} \frac{1}{l^{1+(8/n)}}$$

Considered as a function of the variable $\xi = 1 + (8/n)$, this function has a simple pole with residue unity at $\xi = 1$ (see reference 8). In fact

$$\frac{8}{n} \sum_{l=1}^{\infty} \frac{1}{l^{1+(8/n)}} = 1 + \frac{8\gamma}{n} + 0\left(\frac{1}{n^2}\right) \qquad \text{as } n \to \infty$$

where γ = Euler's constant. Thus

$$m_{33} = \frac{\pi}{2} \rho b^4 \left[1 - \frac{8 \log 2}{n} + 0\left(\frac{1}{n^2}\right) \right] \qquad \text{as } n \to \infty \qquad (29)$$

The value for $n = 3$ was calculated to be $m_{33} = 0.533\, \rho b^4$.

Interpreted in terms of the roll damping (see reference 1) of a slender rocket or missile with n equal, equally spaced fins, we have:

$$\frac{C_{lp}}{(C_{lp})_{n=\infty}} = \frac{m_{33}}{(m_{33})_{n=\infty}}$$

A plot of this function is given in Fig. 3.

References

[1] Bryson, A. E., Jr., *Stability Derivatives for a Slender Missile with Application to a Wing-Body-Vertical Tail Configuration*, Journal of the Aeronautical Sciences, Vol. 20, No. 5, pp. 297–308, May, 1953.

[2] Lamb, H., *Hydrodynamics;* 6th Ed., Dover, N.Y., Ch. VI.

[3] Ward, G. N., *Supersonic Flow Past Slender Pointed Bodies*, Quart. Jour. App. Math. and Mech., Vol. II, Pt. I, 1949.

[4] Milne-Thompson, L. M., *Theoretical Hydrodynamics;* 2nd Ed., Macmillan, N.Y., Ch. IX.

[5] Summers, R. C., *On Determining the Apparent Additional Mass of a Wing-Body-Vertical-Tail Cross Section*, Journal of the Aeronautical Sciences, Vol. 20, No. 12, pp. 856–857, December, 1953.

[6] Bryson, A. E., Jr., *Comment on the Stability Derivatives of a Wing-Body-Vertical Tail Configuration, Journal of the Aeronautical Sciences*, Reader's Forum, Vol. 21, No. 1, p. 59, January, 1954.

[7] Miles, J. W., *On Interference Factors for Finned Bodies*, Journal of the Aeronautical Sciences, Vol. 19, No. 4, p. 287, April, 1952.

[8] Copson, E. T., *Theory of Functions of a Complex Variable;* Oxford Univ. Press, London, 1935, pp. 247–251 and pp. 101–102.

[9] Graham, E. W., *A Limiting Case for Missile Rolling Moments*, Journal of the Aeronautical Sciences, Vol. 18, No. 9, pp. 624–628, September 1951.

Erratum—"Analysis of Stiffened Curved Panels Under Shear and Compression"[1]

M. A. Melcon and A. F. Ensrud
California Division, Lockheed Aircraft Corporation

April 4, 1954

IT HAS BEEN CALLED to our attention that there is a misprint in Eq. (7) of our above-mentioned article. The exponent 1.125 should be 1.25.

Reference

[1] Journal of the Aeronautical Sciences, Vol. 20, No. 2, p. 114, February, 1953.

On Solving Subsonic Unsteady Flow Lifting Surface Problems by Separating Variables

J. W. Miles
Associate Professor of Engineering, University of California, Los Angeles

February 8, 1954

IN A RECENT PAPER dealing with the subsonic unsteady flow over a lifting surface, Professor Kuessner[1] has advocated the development of "new orthogonal coordinate systems and new corresponding functions" in order to "put the problem on the strong shoulders of the mathematician." It is possible that this statement may lead to undue optimism, and it therefore seems pertinent to point out that the problem of solving the Helmholtz equation

$$\nabla^2\phi + \kappa^2\phi = 0 \qquad (1)$$

by separation of variables has been definitively studied by Robertson[2] and Eisenhart,[3] who have shown that separation is possible only in eleven (Euclidean) coordinate systems, viz., (1) rectangular, (2) circular cylinder, (3) elliptic cylinder, (4) parabolic cylinder, (5) spherical, (6) conical, (7) parabolic, (8) prolate spheroidal, (9) oblate spheroidal, (10) ellipsoidal, and (11) paraboloidal.